International Journal of Latest Trends in Engineering and Technology
Special Issue - International Conference on Nanotechnology: The Fruition of Science-2017, *pp.144-150*
e-ISSN:2278-621X, p-ISSN: 2319-3778

INTERATOMIC BONDING AND CHARGE ORDERING IN SUPERPRAMAGNETIC LA0.8ZN0.2FEO3 MULTIFERROIC

G.Gowri[1], R.Saravanan[2]

Abstract-In this work, Zinc doped LaFeO3 multiferroic (La0.8Zn0.2FeO3) has been synthesized by chemical co-precipitation method. An attempt to characterize the bonding and visualization of the charge ordering between the nearest neighbouring atoms in the unit cell of La0.8Zn0.2FeO3 is acheived using maximum entropy method (MEM). The prepared sample has been characterized using powder X-ray diffractometer, transmission electron microscope, UV-Visible spectrometer and vibration sample magnetometer (VSM) to study its crystal structure, surface morphology, optical and magnetic properties respectively. The structural analysis has been done on the experimental powder X-ray diffraction data using Rietveld refinement technique and the structure factors obtained from the refinement process have been used to analyze 3D, 2D and 1D electron density distributions. From the 2D contour maps and the 1D electron density line profiles the information about the charge ordering, nature of bonding and the bond strength of the Fe–O1 and the La–O1 bond in the unit cell of La0.8Zn0.2FeO3 are investigated. The average crystallite size has been calculated using powder X-ray diffraction data using Scherrer formula. The average particle size has been determined using TEM images. The optical band gap energy of prepared sample has been estimated through UV-Visible spectrum. The magnetic parameters are extracted from the hysteresis loop recorded at the room temperature using vibration sample magnetometer. The low value of coercivity, moderately high value of magnetization and the shape of the M-H loop suggests the superparamagnetic behaviour of the sample. As the prepared sample possesses considerably high value of magnetization and low value of coercivity it would be quite interesting in different switching as well as in other multifunctional devices such as spintronic sensors.

Keywords:XRD, MEM, charge ordering, UV-Visible analysis, Coercivity.

1. INTRODUCTION

Now-a-days the multiferroic materials have drawn much attention of the researchers due to their promising applications in numerous advanced technologies such as data storage media, spintronic devices, multiple storage memories and sensors [1-3]. $LaFeO_3$ is a multiferroic material and has the structure similar to ABO_3. In ABO_3 perovskite materials, the smaller cations B are at the centre of the octahedron of oxygen anions and the large cations A are at the corners of the unit cell [3,4]. The compound $LaFeO_3$ crystallizes in an orthorhombically distorted perovskite oxide with a space group P*nma*, which is derived from the standard cubic structure through the distortion of the BO_6 octahedra [5-7]. Since $LaFeO_3$ has interesting properties like, wide-gapped antiferromagnetic insulator with high Néel temperature (T_N~740°C) [8], coexistence of coupled ferroelectric and antiferromagnetic ordering etc.[9], it is considered as a significant material among the rare earth orthoferrite series. In $LaFeO_3$ an induced electrical polarization and magnetization can be controlled by applying magnetic field and and electric field respectively. Due to this effect it can be used in the construction of spin valves with functionality that is tunable by an electric field, novel spintronic devices such as tunneling magnetoresistance (TMR) sensors, [10], and multistate memories in which data are written electrically and read magnetically [11-13]. Though, the pure and doped lanthanum ferric oxide can be prepared by various process like microwave synthesis [14-16], solid state reaction method [17], hydrothermal method [18-20], the chemical co-precipitation method [21] etc., the chemical co-precipitation method is the most attractive one because it is cost effective. Research on pure and doped lanthanum orthoferrite reveals that their structural, electrical, magnetic properties effectively depend on their stoichiometry, cationic substitution, synthesis and processing of its precursor powder. It has been already reported that Zn^{2+} doping at La^{3+} site in $LaFeO_3$, alters its magnetic behaviour and the magnetization of $La_{1-x}Zn_xFeO_3$ (x =0.1, 0.3) multiferroics were found to be increased with the increase in dopant concentration [21].

The main objective of the authors is focused on the investigation regarding the charge density distribution and also the bond strength between the atoms in the unit cell of multiferric materials, by employing the maximum entropy method (MEM) from which numerical value of charge density could be evaluated.

Thus in this work, we have prepared $La_{0.8}Zn_{0.2}FeO_3$ multiferroic using the chemical co-precipitation method and have investigated the charge ordering and also the bond strength between the atoms in the unit cell that are responsible for their optical and magnetic properties.

2. EXPERIMENTAL PROCEDURE

2.1 SAMPLE PREPARATION

The multiferroic $La_{0.8}Zn_{0.2}FeO_3$ was prepared by the chemical co-precipitation method. High purity oxides La_2O_3 (99.99 %, Alfa Aesar), ZnO (99.99 %, Alfa Aesar) and Fe_2O_3 (99.99 %, Alfa Aesar) in the desired stoichiometric proportions were weighted and each oxide was taken in a beaker. With this required amount of distilled water was added followed by

[1] *Research centre and Post Graduate Department of Physics, The Madura College, Madurai-625011, Tamil Nadu, India.*
[2] *Research centre and Post Graduate Department of Physics, The Madura College, Madurai-625011, Tamil Nadu, India.*

the dropwise addition of concentrated nitric acid until a clear salt solution was obtained. Then these solutions were taken in a single beaker and were ultrasonicated for about 2h. With this solution 0.4 N NaOH solution was added dropwise until its PH reaches ~9. The co-precipitated particles were heated at 80°C with rigorous stirring by a magnetic stirrer for 2h. Finally, these co-precipitated particles were washed with water, filtered and dried at 100°C for 12h. The final product was pre-calcined in the air at 400°C for 3h. The precursor was made into circular pellets of 12 mm in diameter and 1mm thickness and then sintered at temperature of 900°C for 2h, to obtain the $La_{0.8}Zn_{0.2}FeO_3$ multiferroic.

2.2 CHARACTERIZATION TECHNIQUES

The X-ray diffraction pattern of the prepared multiferroic was recorded using X-ray diffractometer, (Bruker AXS D8 Advance), at sophisticated analytical instrument facility (SAIF), Cochin university, Cochin, India. The X-ray diffraction data were measured in the 2θ range of 5°-120° with the step size of 0.02°, with CuK_α monochromatic beam of wavelength λ=1.54056 Å. TEM images were recorded with different magnification using Transmission Electron Microscope (TEM) Jeol/JEM 2100 at SAIF, Cochin, India. The optical absorption spectrum of the sample was recorded using UV-visible –NIR spectrometer, (Varian Cary 5000), at SAIF, Cochin, India. The magnetic hysteresis loop was traced using vibration sample magnetometer (Lakeshore VSM 7410) at SAIF, Indian Institute of Technology of Madras, Chennai, India

3. RESULTS AND DISCUSSIONS

3.1 STRUCTURAL ANALYSIS

Figure 1 shows the raw XRD powder pattern of the prepared multiferroic. The observed X-ray peaks for the prepared sample were matched well with the peaks of $LaFeO_3$ phase reported in the JCPDS file (No.37-1493). The XRD pattern confirms that the product is a perovskite oxide with orthorhombic structure with the space group of P*nma* (No.62). Two additional peaks have been identified and matched with the peaks of La_2O_3 exhibiting cubic structure with the space group I*a*-3 reported in the JCPDS file (No.22-0369). The additional peaks due to La_2O_3 are shown in Figure 1. To analyze the structural parameters of the prepared multiferroic its experimental X-ray diffraction data were subjected to the Rietveld refinement technique [22], which is employed in the software JANA 2006 [23]. The Rietveld refinement [24] is the standard tool which was devised by Hugo Rietveld [22] for use in the characterization of crystalline materials. The Rietveld [22] method has been used to fit the theoretically modelled profile with the observed one.

With the experimental powder XRD data, the structural refinement was done taking into account orthorhombic structure for $La_{0.8}Zn_{0.2}FeO_3$ multiferroic having the space group of P*nma* with 4 molecules per unit cell. The refined profile for the prepared multiferroic is shown in Figure 2. The refined structural parameters and the reliability indices are given in Table 1.

The average crystallite size of the prepared multiferroic was calculated using the grain software [25] with full width at half maximum (FWHM) and Bragg angle of the prominent intensity peaks obtained from the experimental powder XRD data. The grain software employs Scherrer formula $t = 0.9\lambda/\beta\cos\theta$, where t is grain size, λ is wavelength of X-ray (λ=1.54056 Å), β is the full width at half maximum in radian and θ is the Bragg angle. The average crystallite size of the prepared multiferroic is 15.8 nm

3.2 CHARGE DENSITY ANALYSIS

The maximum entropy method (MEM) which is a statistical approach proposed by Collins [26], is a great tool to study the electronic structure of the materials. To construct the charge ordering around the atoms and hence to understand the nature and the strength of chemical bond between the neighbouring atoms in the unit cell of the prepared sample, the maximum entropy method (MEM) was used. For the MEM procedure the refined structural parameters evolved from the Rietveld refinement technique were utilized. The software PRIMA (Practice of Iterative MEM Analysis) [27], which employs the Maximum Entropy Method technique was used to estimate the charge density of the sample and the resultant charge density distribution has been mapped and visualized using the visualization software VESTA (Visualization for Electronic and STructural Analysis) [28]. In this work the MEM refinement was carried out by dividing the unit cell into 48 x 72 x 48 pixels. The obtained parameters from the charge density refinement using MEM have been given in Table 2.

For the prepared multiferroic, the three dimensional electron density distribution in the unit cell with an isosurface level of 3 e/$Å^3$ is shown in Figure 3. The 3D charge density distribution clearly gives the position of the La, Fe and O atoms in the unit cell and confirms the orthorhombic phase of the prepared $La_{0.8}Zn_{0.2}FeO_3$ multiferroic. The shaded region enclosed by the electron cloud illustrates an atom. The bond length obtained from MEM is given in Table 3.

The 3D unit cell of $La_{0.8}Zn_{0.2}FeO_3$ with shaded (100) plane is shown in Figure 4(a) and 4(b) depicts the two dimensional charge density map showing Fe-O_1 bond on the (100) miller plane. Similarly, Figure 5(a) shows the 3D unit cell with (200) plane shaded and 5(b) depicts the two dimensional charge density map showing La-O_1 bond on the (200) miller plane. From the 2D charge density maps, it is clearly seen that the contour lines are elongated from Fe to O_1 atom and also from La to O_1 atom. The elongation of contour lines indicates the accumulation of charges towards the bonding region that arises due to the sharing of electrons. Thus the 2D maps illustrate both the bonds Fe-O_1 and La-O_1 are highly covalent.

To understand the electron density distribution and the bonding nature more clearly, the one dimensional charge density profiles corresponding to the Fe-O_1 and La-O_1 bonds are drawn as shown in Figure 6(a) and 6(b). The value of the charge density at the bond critical point along the Fe-O_1 bond and the La-O_1 bond is estimated and is given in Table 3. In the

prepared multiferroic, the high value of charge density estimated at the bond critical point of the Fe-O_1 and La-O_1 bonds declare that both the bonds are predominantly covalent.

3.3 TEM ANALYSIS

The particle size and the surface morphology of the prepared $La_{0.8}Zn_{0.2}FeO_3$ multiferroic, were investigated through TEM images taken with different magnification using Transmission Electron Microscope.

Figure 7 illustates the TEM micrograph of $La_{0.8}Zn_{0.2}FeO_3$ multiferroic along with the corresponding selected area electron diffraction (SAED) pattern. The selected area electron diffraction pattern signifies the polycrystalline nature of the sample. From the TEM image, it can be seen that the particles are uneven in shape and they seems to be irregularly agglomerated. An overview of the TEM images of the prepared multiferroic shows that the particles have a size distribution of approximately 595 nm.

3.4 UV-VISIBLE ANALYSIS.

The optical properties of the prepared $La_{0.8}Zn_{0.2}FeO_3$ multiferroic were studied using UV-Visible absorption spectrum which shows strong absorption peak in the UV-region at the wavelength approximately 353 nm. The band gap energy (E_g) of the prepared sample is determined using the Tauc's equation that relates the absorption coeffecient and the energy band gap of the material as $(\alpha h\nu) = A\,(h\nu - E_g)^n$ [29], where α is absorption coefficient, $h\nu$ is photon energy (E), A is a material constant, E_g is the energy band gap and n is 1/2, as $LaFeO_3$ system is a direct band gap material. To estimate the energy band gap of the prepared sample a graph is drawn with $(\alpha E)^2$ versus energy as shown in Figure 8, where the extrapolation of the tangent of the curve to the zero value of $(\alpha E)^2$ gives the value of E_g as 2.1032 eV.

3.5 MAGNETIC BEHAVIOUR ANALYSIS

To analyze the magnetic properties of the prepared multiferroic the magnetic hysteresis loop has been recorded at room temperature by subjecting the sample to the magnetic field of 20KG using a vibration sample magnetometer. The hysteresis loop, which shows the variation of magnetization as a function of an applied magnetic field is shown in Figure 9. The values of coercivity, maximum magnetization and remanent magnetization extracted from the hysteresis loop are 5.2156 G, 0.8427 emu/g, 0.0019 emu/g respectively. The sigmoidal shape of magnetization curve without any loop with a small coercivity and almost zero remanence reveals the superparamagnetic behaviour of the sample. It has been reported earlier that the maximum magnetization value of pure $LaFeO_3$ system is 0.485 emu/g [21]. The maximum magnetization value for the prepared $La_{0.8}Zn_{0.2}FeO_3$ multiferroic is found to be high as 0.8427 emu/g. Thus the substitution of Zn^{2+} ions in $LaFeO_3$ leaves the system to acheive high magnetization with low coercivity. Since, $La_{0.8}Zn_{0.2}FeO_3$ multiferroic has low coercivity and moderately high value of magnetization, it can be used as a promising candidate in different switching as well as in other multifunctional devices such as spintronic sensors.

4 CONCLUSION

$La_{0.8}Zn_{0.2}FeO_3$ multiferroic was successfully prepared by chemical co-precipitation method. The XRD result confirms the orthorhombic phase of the sample with space group P*nma*. The average crystallite size is estimated using powder X-ray diffraction data by employing Scherrer formula. The refined structure factors obtained from the Rietveld refinement method were used in charge density analysis through MEM. The 2D maps and the estimated charge density value at the bond critical point of Fe-O_1 and La-O_1 bond confirms the covalent nature of both the bond. TEM images show that the particles are uneven in shape and are irregularly agglomerated. The optical analysis was used to find its energy band gap value. The magnetic measurements illustrate that Zn doping in $LaFeO_3$ leaves the system to acheive high magnetization and low coercivity.

ACKNOWLEDGEMENT

The authorities of The Madura College are gratefully acknowledged for their constant encouragement of the research activities of the authors.

REFERENCES

[1] J.F.Scott, Nature Materials 6 (2007) 256.
[2] N.A. Hill, Why are there so few magnetic ferroelectrics? J. Phys. Chem. B, 104 (2000) 6694–6709.
[3] M.Bibes, A. Barthelemy, Nature Materials 7 (2008) 425.
[4] J.-M. Liu, Q.C. Li, X.S. Gao, Y. Yang, X.H. Zhou, X.Y. Chen, et al, Order coupling in ferroelectromagnets as simulated by a Monte Carlo method, Phys. Rev. B, 66, (2002) 054416–054426.
[5] Y.-H. Lee, J.-M. Wu, Epitaxial growth of $LaFeO_3$ thin films by RF magnetron sputtering, J. Cryst. Growth. 263 (2004) 436-441.
[6] P.M. Woodward, Octahedral Tilting in Perovskites. I. Geometrical Considerations, Acta Cryst. B53 (1997) 32-43.
[7] P.M. Woodward, Octahedral Tilting in Perovskites. I. Geometrical Structure, Acta Cryst. B 53 (1997) 44-66.
[8] G.R. Hearne, M.P. Pasternak, Electronic structure and magnetic properties of LaFeO3 at high pressure, Phys. Rev. B. 51 (1995) 11495–11500.
[9] S. Acharya, J. Mondal, S. Ghosh, S.K. Roy, P.K. Chakrabarti, Multiferroic behavior of Lanthanum orthoferrite (LaFeO3), Mater. Lett. 64 (2010) 415-418.
[10] M.Gajek, Nature Materials 6 (2007) 296.
[11] W.Eerenstein, N.D.Mathur, J.F.Scott, Nature 442 (2006) 759
[12] J.F.Scott, F.D.Morrison, M.Miyake., Journal of the American ceramic society 88 (2005) 1691.
[13] M.Dawber,K.M Rabe, J.F.Scott., Reviews of Modern Physics 77 (2005) 1083.
[14] Tang P, Tong Y, Chen H, Cao F, Pan G, Microwave-assisted synthesis of nanoparticulate perovskite $LaFeO_3$ as a high active visible-light photo catalyst, Curr. Appl. Phys. 13, (2013) 340–343.

[15] Farhadi S, Momeni Z, Taherimehr M, Rapid synthesis of perovskite-type LaFeO3 nanoparticles by microwave-assisted decomposition of bimetallic La[Fe(CN)6] 5H2O compound, J. Alloy Compd. 471 (2009) 15–18.
[16] Ding JLX, Shu H, Xie J, Zhang H, Microwave-assisted synthesis of perovskite ReFeO3 (Re: La, Sm, Eu, Gd) photocatalyst, Mater. Sci. Eng. B. 171 (2010) 31–34.
[17] S. Acharya, P.K. Chakrabarti, Some interesting observations on the magnetic and electric properties of Al doped lanthanum orthoferrite ($La_{0.5}Al_{0.5}FeO_3$), Solid State Commun. 150, (2010) 1234-1237.
[18] Thirumalairajan S, Girija K, Ganesh I, Mangalaraj D, Viswanathan C, Balamurugan A, Ponpandian N, Controlled synthesis of perovskite $LaFeO_3$ microsphere composed of nanoparticles via self-assembly process and their associated photo catalytic activity, Chem. Eng. J. 209 (2012) 420–428.
[19] Zheng W, Liu R, Peng D, Meng G, Hydrothermal synthesis of LaFeO3 under carbonate-containing medium , Mater. Lett. 43 (2000) 19–22.
[20] Ji K, Dai H, Deng J, Song L, Xie S, Han W, Glucose-assisted hydrothermal preparation and catalytic performance of porous $LaFeO_3$ for toluene combustion, J. Solid State Chem. 199 (2013) 164–170.
[21] K..Mukhopadhyay, A.S.Mahapatra, P.K.Chakrabarti, Multiferroic behavior, enhanced magnetization and exchange bias effect of Zn substituted nanocrystalline $LaFeO_3$ ($La_{(1-x)}Zn_xFeO_3$, x=0.10, and 0.30), J. Magn. Magn. Mater. 329 (2013) 133–141.
[22] H.M. Rietveld, A Profile Refinement Method for Nuclear and Magnetic Structures, J. Appl. Crystallogr. 2 (1969) 65-71.
[23] Petříček, V., Dušek, & M., Palatinus, L. (2006). JANA 2006, the crystallographic computing system. Praha, Czech Republic, Academy of Sciences of the Czech Republic.
[24] M. M. Wolfson, Introduction to X-ray Crystallography. Cambridge University Press, London, 1970.
[25] R. Saravanan, Grain software (Personal communication) (2008).
[26] D.M.Collins, Electron density images from imperfect data by iterative entropy maximization, Nature. 298 (1982) 49-51.
[27] F.Izumi, R.A.Dilanien, PRIMA, for the maximum entropy method advanced materials laboratory, Japan (2004).
[28] K.Momma and F.Izumi, VESTA: a three-dimensional visualization system for electronic and structural analysis, J.Appl. Crystallogr. 41 (2008) 653.
[29] J.Tauc, R.Grigorovic, A.Vancu, Optical properties and electronic structure of amorphous germanium, Physica Status Solidi. 15, (1966) 627-637.

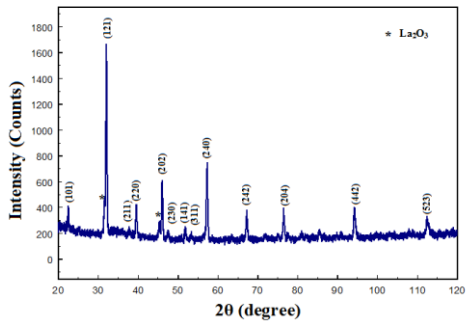

Figure 1 The observed X-ray diffraction pattern of $La_{0.8}Zn_{0.2}FeO_3$

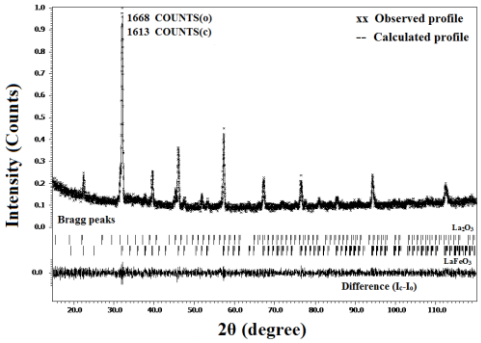

Figure 2 Rietveld refinement profile of $La_{0.8}Zn_{0.2}FeO_3$ mutiferroic

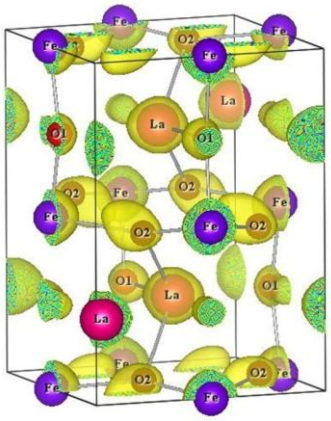

Figure 3 3D charge density distributions of $La_{0.8}Zn_{0.2}FeO_3$ multiferroic

(a) (b)

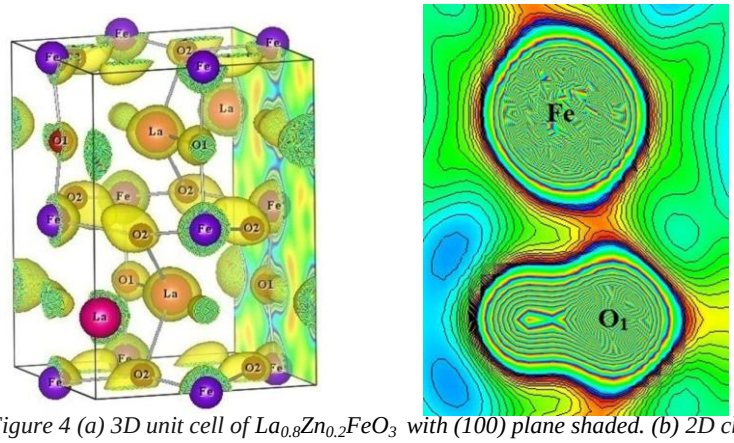

Figure 4 (a) 3D unit cell of $La_{0.8}Zn_{0.2}FeO_3$ with (100) plane shaded. (b) 2D charge density distribution of $La_{0.8}Zn_{0.2}FeO_3$ showing Fe-O_1 bond on the (100) plane. Contour lines are drawn between 0 and 1 e/Å^3 with 0.06 e/Å^3 interval.

(a) (b)

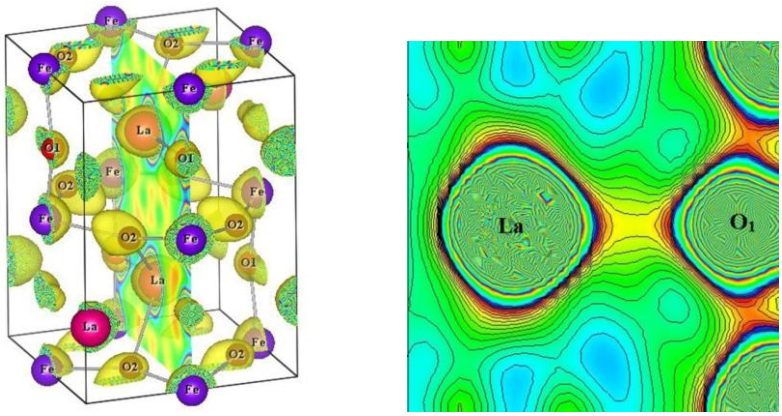

Figure 5 (a) 3D unit cell of $La_{0.8}Zn_{0.2}FeO_3$ with (200) plane shaded. (b) 2D charge density distribution of $La_{0.8}Zn_{0.2}FeO_3$ showing La-O_1 bond on the (200) plane. Contour lines are drawn between 0 and 1.2 e/Å^3 with 0.06 e/Å^3 interval.

(a)

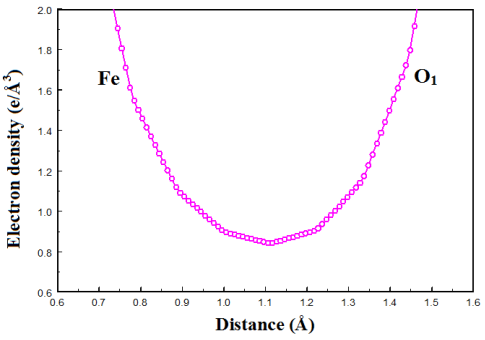

(b)

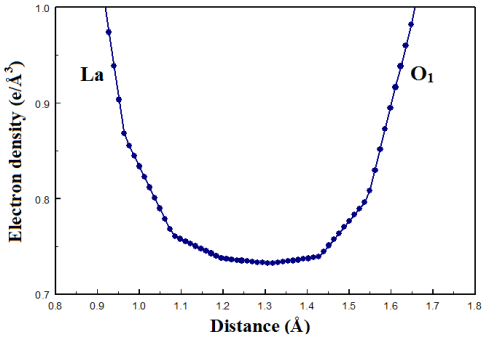

Figure 6 1D electron density profiles between (a) Fe and O_1 atoms (b) La and O_1 atoms in the unit cell of $La_{0.8}Zn_{0.2}FeO_3$.

(a) (b)

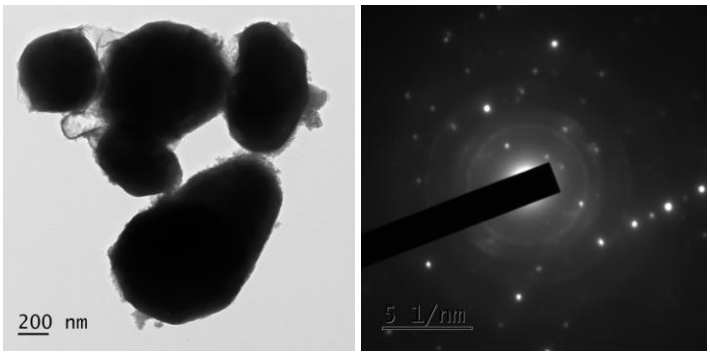

Figure 7 (a) TEM image (b) SAED pattern of $La_{0.8}Zn_{0.2}FeO_3$ multiferroic

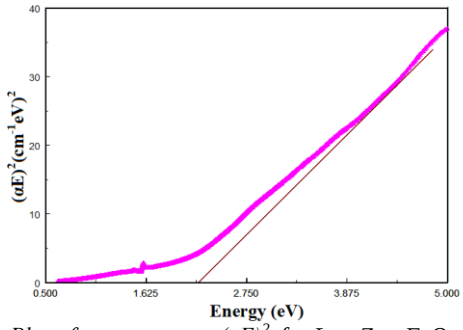

Figure 8 Plot of energy versus $(\alpha E)^2$ for $La_{0.8}Zn_{0.2}FeO_3$ multiferroic

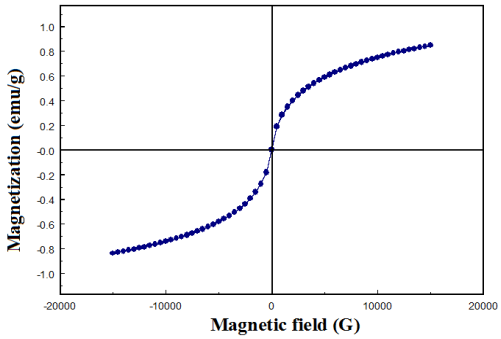

Figure 9 Magnetic hysteresis loop of $La_{0.8}Zn_{0.2}FeO_3$ multiferroic.

Table 1. Structural parameters of $La_{0.8}Zn_{0.2}FeO_3$ multiferroic through refinement of powder XRD data

Parameter	**$LaFeO_3$**
a (Å)	5.5615(6)
b (Å)	7.8460(1)
c (Å)	5.5514(7)
α = β = γ (◦)	90
Cell Volume, V ($Å^3$)	242.2436(76)
Density, ρ (gm/ cc)	6.2508(7)
Observed reliability factor, R_{obs} (%)	3.26
Profile reliability factor, R_P (%)	5.87
Goodness of fit (GOF)	1.05
Number of electrons in the unit cell	406

Table 2. Parameters from MEM refinements of $La_{0.8}Zn_{0.2}FeO_3$ multiferroic

Parameter	**$LaFeO_3$**
Number of pixels in the unit cell (48x72x48)	165888
Number of electrons in the unit cell	406
Lagrangian parameter, λ	0.0140
Number of refinement cycles	1818

Reliability factor, R_{MEM} (%)	2.4248
Weighted reliability factor, $_{W}R_{MEM}$ (%)	2.3811

Table 3. Bond length and charge density at the bond critical point between atoms in $La_{0.8}Zn_{0.2}FeO_3$ multiferroic

Bond	**Distance (Å)**	**Charge density (e/Å^3)**	**Bond length (Å)**
Fe-O_1	1.1164	0.8448	2.0015
La-O_1	1.3183	0.7323	2.4292